Production of nano Zero Valent Iron particles by Means of a Spinning Disk Reactor

Giorgio Vilardi*, Marco Stoller, Nicola Verdone, Luca Di Palma

Sapienza University of Rome, Dept. Of Chemical Materials Environmental Engineering Via Eudossiana 18, 00184 Rome, Italy
giorgio.vilardi@uniroma1.it

Nitrates are considered hazard compounds for human health due to their tendency to be reduced to nitrites, in particular in reducing environment. Nano zero valent iron (nZVI) represents an efficient and low-cost adsorbent/reductive agent for nitrate removal from groundwater. In this work, nZVI particles were produced by means of two different equipment types based on the same chemical synthesis method: a batch stirred tank reactor (BSTR) and a spinning disk reactor (SDR). This latter apparatus is capable to strongly promote micromixing at a steady-state, continuous condition, and such as qualifies to subsist in the framework of process intensification. Particle size distribution (PSD) of the obtained nZVI particles were measured by a DLS technique. The removal efficiency of the produced nVI particles were checked by using two NO_3^- solutions (1.6 and 6.4 mM) and by monitoring nitrate concentration reduction rates at selected time intervals. Results showed that the nZVI particles produced by SDR have a narrow PSD with a mean diameter of 65nm; on the contrary, particles produced by BSTR shows bimodal PSD with modal sizes of 105 nm and 400 nm, respectively. Experimental tests of nitrates reduction in water have been performed, using both the particles produced by the above mentioned techniques. Results of batch tests showed that the highest removal efficiency of nitrates was observed by using the nZVI particles produced by means of SDR, as a consequence of the higher average specific surface. Since nitrate removal process involves both reduction and adsorption processes, the removal mechanism has been investigated, and the pseudo-first-order reduction kinetic model was successfully tested and reported in both cases.

1. Introduction

Due to the growing interest in the applied nanotechnology in several fields (environmental, industrial and civil ones) an increasing demand of controlled-size and shape particles was observed in the last twenty years (Bavasso et al., 2016). Innovative equipment and processes, which grant a significant improvement in the chemical production industry, compared to those used today, have developed a novel philosophy early based on the reduction capital cost involved in a particular production system (Dautzenberg and Mukherjee, 2001). All of these developments share a common focus on ''Process Intensification'' an approach which leads to go beyond ''traditional'' chemical engineering and which has as main purpose the development of new equipment, strategies and processes in order to achieve a substantially smaller, cleaner and more energy-efficient technology (Stankiewicz and Moulijn, 2000; Di Palma and Verdone, 2009).

Spinning Disk Reactor (SDR) represents a successful technology for the continuous production of nanoparticles by wet chemical synthesis and grants the synthesis of products characterized by a narrow and uniform size distribution (de Caprariis et al., 2012). As already reported in previous studies, SDR was a suitable device for the development of more efficient and faster chemical synthesis based on the chemical precipitation method (D'Intino et al, 2014). SDR has been already used for the production of titanium dioxide nanoparticles (Stoller et al., 2009) and hydroxyapatite nanoparticles (Parisi et al., 2011; de Caprariis et al., 2015). To obtain particles at nano-scale the attainment of local micro-mixing conditions in the reaction volume of the vessel is mandatory; SDR, compared with T-mixer, seems to be more profitable due to the involvement of a much smaller specific energy consumption (Cafiero et al., 2002). The rotation of disk surface at high speed (200-6000 rpm, depending on the diameter of the disk) induces high centrifugal fields which grant the

formation of a liquid film characterized by a thickness of 0.05-0.5 mm. Thus, the main benefit of the SDR is the mass transfer improvement followed by a significant reduction of the mixing time and the possibility to produce nanoparticles in continuous. Another benefit is the ease of industrial scaling-up of the device.

Nano zero valent iron (nZVI) particles have been synthetized in batch stirred tank reactor by authors (Di Palma et al., 2015a) by the classical borohydride reduction method (Glavee et al., 1995). Thus, the top-down approach was selected, which results more suitable for a lab-scale production in comparison with the bottom-up approach, which requires a mechanical size reduction of micrometric iron which could originates from End of Life Vehicles shredding (Di Palma et al., 2015b). The nanoparticles produced are characterized by a large specific surface area, high chemical reactivity and the capacity to remain in suspension as colloidal dispersion for several hours, due to the use of a dispersing agent, such as carboxymethylcellulose (He and Zhao, 2007). nZVI represents the most versatile agent for the removal of both organic and inorganic pollutants, such as heavy metals (Gueye et al., 2016), respect to other chemical treatments (Marsili et al., 2007; Stoller et al., 2016) and inorganic anions, such as nitrates (Muradova et al., 2016). The latter chemical species, NO_3^-, is considered an hazardous compound for human health, due to the possibility of its reduction to nitrite in the stomach and the subsequent oxidation of haemoglobin-bounded-Fe(II) to Fe(III), which produce methemoglobin, a metalloprotein which in the heme group brings a ferric ion and is not able to carry oxygen or carbon dioxide (Vilardi and Di Palma, 2016). The main nitrogen compounds sources are septic waste, animal manure, leachate from landfill and the over-fertilization of soils. In particular, among the different inorganic N-based compounds, nitrates are the most diffuse and are characterized by a high chemical stability (highest oxidative state of N) and solubility. nZVI has demonstrated high efficacy for the nitrate treatment also at high concentration (Sparis et al., 2012) and the main products of the reaction are ammonia and oxyhydroxide of Fe(II) and Fe(III). In this study a comparison between the production of nZVI particles in batch (BSTR-nZVI) and in continuous (SDR-nZVI) by means of a SDR is reported, with respect to the mean hydrodynamic diameter and size distribution obtained. Furthermore, the nitrates removal efficiency in synthetic aqueous solutions was investigated using the SDR-nZVI and BSTR-nZVI. A kinetic study was also reported. To the best of our knowledge this is the first work which deals with the production of nZVI by means of a SDR.

2. Materials and methods

All reagents used were of analytical grade (ACS) and were purchased from Sigma Aldrich, Milan. A schematic representation of the SDR used for the production of nZVI particles is reported in Figure 1 (de Caprariis et al., 2015).
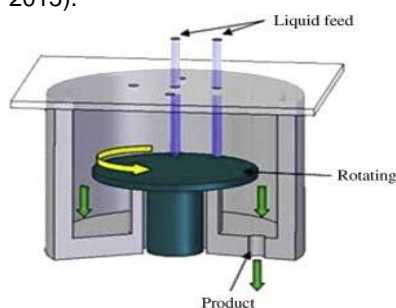
Figure 1: Spinning Disk Reactor

The redox-precipitation reaction between the iron precursor ($FeSO_4 \cdot 7H_2O$) and the reducing agent ($NaBH_4$) took place on an inner disk of 8.5 cm in diameter. The product was continuously removed from the bottom of the reactor. The two reagent solutions were injected over the disc at three different distances (4, 3 and 2 cm) and the two injection positions were placed at the same distance of 2 cm from the center of the disk to achieve more easily micro-mixing efficiency (Cafiero et al., 2002). The first reagent solution (A) is an aqueous solution of $FeSO_4 \cdot 7H_2O$ 40 mM, whereas the second reagent solution (B) is an aqueous solution of $NaBH_4$ 80 mM, adopting a stoichiometric molar ratio $BH_4^-/Fe(II)=2$, according to the following reaction (Vilardi and Di Palma, 2016):

$$2BH_4^- + Fe(H_2O)^{2+} \rightarrow Fe(0) + 2B(OH)_3 + 7H_2 \uparrow \qquad (1)$$

These solutions are fed in two steps: first only the reagent A was injected to create the liquid film all over the disc. Once the film is created, the reagent B was injected. No inert gas was supplied during the process and no buffer systems or temperature control were adopted. In order to optimize the production of nanoparticles, only the injection position-disk centre distance (2 cm) and rotational velocity (146.5 rad s^{-1} according to de

Caprariis et al., 2012) were fixed, while the injection distance over the disk (H) and the flow rate of the two reagents, Q_A for reagent A and Q_B for reagent B, were varied. In particular, Q_A was varied in the range 100-150 mL min^{-1}, whereas Q_B was varied in the range 25-50 mL min^{-1}. Seven runs were carried out in three steps: initially fixing Q_B=37.5 mL min^{-1} and H equal to 4 cm, setting Q_A equal to 200, 175 and 150 mL min^{-1}. In the second step the optimum Q_A was chosen and Q_B was set equal to 25 and 50 mL min^{-1}. In the third and final step optimum Q_A and Q_B were fixed, while the value of H was set equal to 3 and 2 cm, respectively. The optimum process parameters were evaluated by measuring the produced particle size distribution (PSD) by the instrument Plus 90 supplied by Brookhaven.

As regards the second experimental set-up, a batch stirred tank reactor (BSTR) was adopted. The synthesis followed was carried out according to previous studies (Di Palma et al., 2015b; Gueye et al., 2016; Vilardi and Di Palma 2016). The produced nanoparticles were then used in the nitrate reduction in aqueous solution, to compare the efficiency of the two series of nanoparticles. In brief, removal nitrates experiments were carried out in a 250 mL conical flask on a shaker at 25°C. $NaNO_3$ was the model contaminant. Two nitrate solutions (1.6 and 6.4 mM of NO_3^-) were tested to investigate the reaction kinetic of nitrates by sampling about 2 mL of solution at selected time intervals (0, 15, 30, 45, 60, 75, 90, 105, 120 min). The samples were then filtered through a 0.45 mm Whatman membrane filter and diluted to 10 mL with deionized water. Nitrates concentration was measured by ion chromatography (Dionex ICS—1100). The nZVI loading was fixed at stoichiometric amount according to the following reaction (Sparis et al., 2012):

$$4Fe(0) + NO_3^- + 7H_2O \rightarrow 4Fe(II) + NH_4^+ + 10OH^- \tag{2}$$
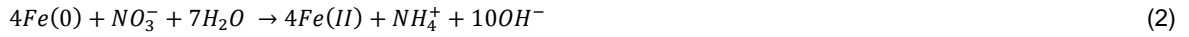
All the experiments were conducted in triplicates to ensure repeatability and accuracy: the mean values are reported.

3. Results and Discussion

3.1 Optimization of the nZVI production by means of a SDR

The main purpose of this work was to start an optimization process of the nZVI synthesis focusing on a continuous production of the nanoparticles by a lab-scale SDR, which represents a perfect equipment for the subsequent industrial scale-up. The effect of the reagents feeding mode was investigated and the fixed parameters and obtained results are reported in Table 1.

Table 1: Experimental results and operating parameters

Run	H (cm)	Q_A (mL min^{-1})	Q_B (mL min^{-1})	d_m (nm)
1	4	200	37.5	94
2	4	175	37.5	87
3	4	150	37.5	70
4	4	150	25	75
5	4	150	50	80
6	3	150	37.5	68
7	2	150	37.5	65

In Table 1, H is the distance of the injection point over the disk whereas d_m is the mean hydrodynamic diameter of the nanoparticles produced. As it is possible to observe decreasing the flow rate of the reagent A, which creates the liquid film on the disk surface, produces a significant decrease of the mean size of the nanoparticles, from 94 nm to 70 nm. A possible explanation of this result is based on the relation between the flow-rate of the solution, which creates the liquid film, and the thickness of the film. Indeed, the thickness of the liquid film is strongly dependent on the disk diameter, on the rotational velocity, on the radial distance of the injection point, on the physical properties of the solution and on its flow-rate. In these experiments only the latter parameter was varied, and according to the following equation (3) a decrease in the flow rate produces a decrease in the thickness of the film:

$$\delta = \left(\frac{3vQ}{2\pi r^2 \omega^2}\right)^{1/3} \tag{3}$$

where ω (rad s^{-1}) is the rotational velocity, r (m) is the radial distance of the injection point, Q (m^3 s^{-1}) the flow-rate and v (m^2 s^{-1}) the kinematic viscosity of the liquid. The mass transfer is foster by a decrease of the film thickness and this improve the diffusion of the nucleation on the disk which results in a less significant agglomeration of the particles produced. Subsequently the optimum Q_A was set to 150 mL min^{-1} and the Q_B

was varied. In the last step, fixing optimum Q_A (150 mL min^{-1}) and optimum Q_B (37.5 mL min^{-1}), the distance of the injection point over the disk was varied. The best result was obtained in the last runs, when the distance between the disk and the two injection points was set to 2 cm. A possible justification of this observation may be that at reduced height H, the impact of the injected reactant flow in the liquid film results to be reduced, and, as a consequence, disturbing less the film integrity and sensibly reducing splashing effects. Moreover, the injected stream is not capable anymore to perforate the thin film, therefore mixing immediately triggers within the liquid film and not at the disk surface, where radial velocities are very low. To deeply investigate the performances achieved, the distribution of the particle's diameter of the last two best runs are reported in Figure 2 and 3, respectively.
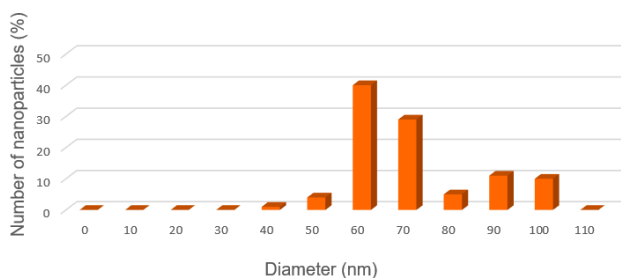
Figure 2: Diameter distribution of the particles obtained in the run 6.
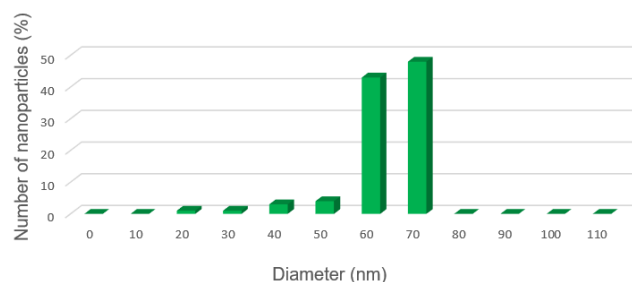
Figure 3: Diameter distribution of the particles obtained in the run 7.

The sixth run yielded a unimodal distribution as the seventh one, but in the latter case no agglomerates were observed. Probably a decrease of the distance between the injection point and the disk surface favours a homogeneous agglomeration of the particles, resulting in a narrower particle size distribution.

3.2 Comparison of nZVI produced by means of BSTR and SDR
To make a comparison between the BSTR and the SDR equipment for the production of nZVI, the distribution diameter of the nanoparticles where reported (Figure 3 shows the case of the SDR production, while Figure 4 shows the case of the BSTR production).
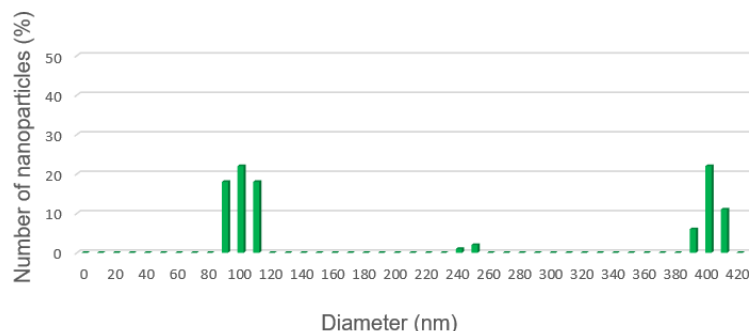
Figure 4: Diameter distribution of the particles produced by means of a BSTR.

As it is possible to observe, the first significant difference is that the mean size of the nanoparticles produced by BSTR is 198 nm, one order of magnitude higher than that of nanoparticles produced by SDR. Furthermore, the BSTR produced several aggregates characterized by a mean diameter of 400 nm, which were classified as micro-cluster and depended on the absence of micro-mixing conditions in the reaction volume. On the

contrary, the SDR permitted to obtain a narrow size distribution and a homogeneous distribution of the nanoparticles in the reaction volume.

3.3 Nitrate removal efficiency and kinetic study

To test and to compare the reactivity of the produced nanoparticles the nitrate removal efficiency was evaluated, varying the initial concentration $[NO_3^-]_0$ of the nitrates. The experimental data were subsequently fitted successfully by the pseudo-first order reduction kinetic, as already reported by other authors (Vilardi and Di Palma, 2016). Figure 5 shows the kinetic reduction of nitrates, according to the following equation:

$$Ln\,([NO_3^-]) = Ln([NO_3^-]) - k_{obs}t \qquad (4)$$

where k_{obs} (min^{-1}) is the observed rate constant of the pseudo-first-order reaction and t (min) is the contact time.
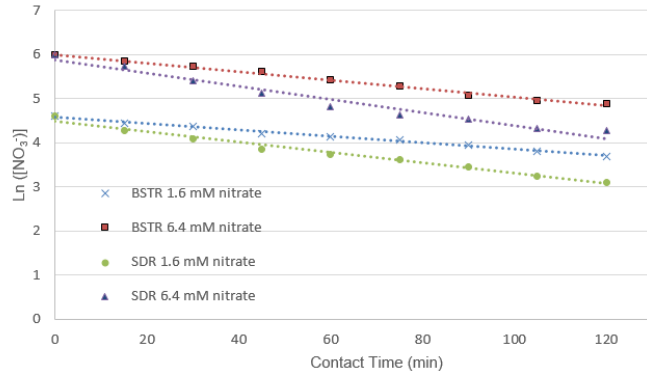
Figure 5: Pseudo-first-order regression lines.

The ZVI nanoparticles produced by means of a SDR showed a remarkable reactivity respect to that produced by a BSTR, independently on the initial concentration of NO_3^-. In both cases in fact the nitrate removal efficiency $\varepsilon(\%)$ resulted higher than 80 %, while in the removal process where the ZVI nanoparticles produced by SDR, ε values resulted less than 70%. In Table 2 the kinetic parameters and the efficiency removal are reported.

Table 2: Kinetic parameters of the nitrate removal process, varying the reactor used and the $[NO_3^-]_0$ value.

Test	k_{obs} (min^{-1})	$t_{1/2}$ (min)	R^2	ε (%)
BSTR ($[NO_3^-]_0$=6.4 mM)	0.0097	71.46	0.99	66.87
BSTR ($[NO_3^-]_0$=1.6 mM)	0.0073	94.95	0.99	60.02
SDR ($[NO_3^-]_0$=6.4 mM)	0.0148	46.83	0.97	81.92
SDR ($[NO_3^-]_0$=1.6 mM)	0.0118	58.74	0.99	77.62

In Table 2 the half life time $t_{1/2}$ (min) where obtained through the following equation:

$$t_{1/2} = \frac{Ln(2)}{k_{obs}} \qquad (5)$$

4. Conclusions

The present work reported for the first time the production of the zero valent iron nanoparticles by means of a SDR. Due to this process intensified equipment it was possible to produce in continuous the nanoparticles, achieving a narrow PSD and reducing significantly the mean size of the particles. Consequently, also the specific surface area of the nanoparticles increased, yielding more reactive nanomaterials for the nitrate removal process. In detail, nZVI produced by means of BSTR and SDR were compared in terms of mean diameter, diameter distribution and nitrate removal efficiency (nZVI reactivity). The former production yielded a bimodal size distribution of the nanoparticles diameters, with two modal size equal to 105 nm and 400 nm respectively, a mean diameter of 198 nm, a nitrate removal efficiency of 60.02 % and 66.87 % at 120 min and a $t_{1/2}$ equal to 94.95 min and 71.46 min in the case of initial nitrate concentrations equal to 1.6 and 6.4 mM, respectively. The SDR production yielded instead a narrow unimodal size distribution, after a first optimization

process, and a mean diameter equal to 65 nm. As regards the nitrate removal process, the reduction seemed to be more efficient and rapid; it was obtained a nitrate removal efficiency of 77.62 % and 81.92 % at 120 min and a $t_{1/2}$ equal to 58.74 min and 46.83 min in the case of initial nitrate concentrations equal to 1.6 and 6.4 mM, respectively. Moreover, the SDR technology allows to develop a fast and efficient industrial scale-up to take the nZVI production on an industrial scale.

References

Bavasso I., Vilardi G., Stoller M., Chianese A., Di Palma L., 2016. Perspectives in nanotechnology based innovative applications for the environment. Chemical Engineering Transactions, 47, 55-60. doi: 10.3303/CET1647010.

Cafiero L. M., Baffi G., Chianese A., Jachuck R. J. J., 2002. Process intensification: precipitation of barium sulfate using a spinning disk reactor. Industrial & engineering chemistry research, 41(21), 5240-5246.

D'Intino A. F., de Caprariis B., Santarelli M. L., Verdone N., Chianese A., 2014. Best operating conditions to produce hydroxyapatite nanoparticles by means of a spinning disc reactor. Frontiers of Chemical Science and Engineering, 8(2), 156-160.

Dautzenberg F. M., Mukherjee M., 2001. Process intensification using multifunctional reactors. Chemical Engineering Science, 56(2), 251-267.

De Caprariis B. Di Rita, M. Stoller, M., Verdone N., Chianese, A., 2012. Reaction-precipitation by a spinning disc reactor: Influence of hydrodynamics on nanoparticles production. Chemical Engineering Science, 76, 73-80.

De Caprariis B., Stoller M., Chianese A., Verdone N., 2015. Cfd model of a spinning disk reactor for nanoparticle production. Chemical Engineering Transactions, 43, 757-762.

Di Palma L., Gueye M. T., Petrucci E., 2015. Hexavalent chromium reduction in contaminated soil: a comparison between ferrous sulphate and nanoscale zero-valent iron. Journal of hazardous materials, 281, 70-76. (a)

Di Palma L., Medici F., Vilardi G., 2015. Artificial Aggregate From non Metallic Automotive Shredder Residue. Chemical Engineering Transactions, 43, 1723-1728. (b) doi: 10.3303/CET1543288

Di Palma L., Verdone N., 2009. The effect of disk rotational speed on oxygen transfer in rotating biological contactors. *Bioresource* Technology, 100, 1467-1470.

Glavee G. N., Klabunde K. J., Sorensen C. M., Hadjipanayis G. C., 1995. Chemistry of borohydride reduction of iron (II) and iron (III) ions in aqueous and nonaqueous media. Formation of nanoscale Fe, FeB, and Fe2B powders. Inorganic Chemistry, 34(1), 28-35.

Gueye M.T., Di Palma L., Allahverdiyeva G., Bavasso I., Petrucci E., Stoller M., Vilardi G., 2016. The influence of heavy metals and organic matter on hexavalent chromium reduction by nano zero valent iron in soil. Chemical Engineering Transactions, 47, 289-294. doi: 10.3303/CET1647049.

He F., Zhao D., 2007. Manipulating the size and dispersibility of zerovalent iron nanoparticles by use of carboxymethyl cellulose stabilizers. Environmental Science & Technology, 41(17), 6216-6221.

Marsili E., Beyenal H., Di Palma L., Merli C., Dohnalkova A., Amonette J. E., Lewandowski Z., 2007. Uranium immobilization by sulfate-reducing biofilms grown on hematite, dolomite, and calcite. Environmental science & technology, 41(24), 8349-8354.

Muradova G., Gadjieva S., Di Palma L., Vilardi G., 2016. Nitrates removal by bimetallic nanoparticles in water. Chemical Engineering Transactions, 47, 205-210. doi: 10.3303/CET1647035.

Parisi M.P., Stoller M., Chianese A., 2011. Production of nanoparticles of hydroxy apatite by using a rotating disk reactor. Chemical Engineering Transactions, 24, 211-216.

Sparis D., Mystrioti, C., Xenidis A., Papassiopi N., 2013. Reduction of nitrate by copper-coated ZVI nanoparticles. Desalination and Water Treatment, 51(13-15), 2926-2933.

Stankiewicz A. I., Moulijn J. A., 2000. Process intensification: transforming chemical engineering. Chemical Engineering Progress, 96(1), 22-34.

Stoller M., Miranda L., Chianese A., 2009. Optimal feed location in a spinning disc reactor for the production of TiO2 nanoparticles. Chemical Engineering Transactions, 17, 993-998.

Stoller M., Azizova G., Mammadova A., Vilardi G., Di Palma L., Chianese A., 2016. Treatment of Olive Oil Processing Wastewater by Ultrafiltration, Nanofiltration, Reverse Osmosis and Biofiltration. Chemical Engineering Transactions, 47, 409–414. doi:10.3303/CET1647069.

Vilardi G., Di Palma L., 2017. Kinetic Study of Nitrate Removal from Aqueous Solutions Using Copper-Coated Iron Nanoparticles. Bulletin of Environmental Contamination and Toxicology, 98: 359. doi:10.1007/s00128-016-1865-9.